ASPS Conference Proceedings 1: 229-237 (2022)

Proceedings of

12th Structural Engineering Convention - An International Event (SEC 2022)

Available at https://asps-journals.com/index.php/acp

Nonlinear Static Pushover Analysis of Hollow Shear Critical RC Bridge Piers Under Monotonic Loading: A Comparitive Study

Vijay Kumar Polimeru[1,*], Arghadeep Laskar[2]

[1] Department of Civil Engineering, Research Scholar, IIT Bombay, Mumbai 400076, India
[2]Department of Civil Engineering, Assistant Professor, IIT Bombay, Mumbai 400076, India, Email: laskar@civil.iitb.ac.in

Paper ID - 030072

Abstract

Hollow RC bridge piers exhibit several failure modes when subjected to extensive time varying loads during their service lives. Shear failure of hollow RC bridge piers is very critical as it is brittle in nature involving rapid deterioration of strength with increasing widths of the shear cracks and low ductility. Hence this type of failure is not desirable in the earthquake prone areas. Simulation models that can accurately predict the characteristic load deflection curve parameters (including yield load, peak load, ultimate load and corresponding drift, ductility and post peak strength degradation) are very much essential for efficient design of these structures. In the present study, a nonlinear static pushover analysis of three hollow rectangular RC bridge piers (one flexure critical and two shear critical) has been performed under monotonic loading using four different analysis techniques. The first type of simulation model used in the present study is based on the commonly used fiber based nonlinear beam-column elements with simple uniaxial material constitutive relationships, which are very effective in predicting the flexural response of bridge piers. The second type of simulation model used in the present study is also based on simple fiber based nonlinear beam-column elements. However, the constitutive relationships of steel in this model are modified to predict the post-peak strength degradation in shear critical bridge piers. The third type of simulation model is based on two dimensional (2D) CSMM based smeared RC plane stress elements. The fourth type of simulation model is an analytical model based on the sectional analysis method. The load deflection curve properties obtained from all the simulation models have been compared with each other and also with the experimental data. It has been concluded from the present study that all four models are equally efficient in predicting the behaviour of flexure critical bridge pier. However, in the case of shear critical bridge piers, predictions from the 2D CSMM based simulation model are more accurate.

Keywords:Nonlinear Static Pushover Analysis, RC Hollow Rectangular Bridge Piers, Cyclic Softened Membrane Model (CSMM), Monotonic Loading, Hysteretic Steel, Analytical Model.

1. Introduction

Hollow RC bridge piers exhibit several failure modes when subjected to extensive time varying loads during their service lives. Shear failure of hollow RC bridge piers is very critical [1] as it is brittle in nature involving rapid deterioration of strength with increasing widths of the shear cracks, low ductility and energy dissipation capacities. Hence this type of failure is not preferable in the earthquake prone areas. Accurate simulation models which can predict the complete nonlinear behavior (elastic, inelastic and post peak failure range) of these structures are essential to study their performance under seismic loads [2]. Simulation models that can accurately predict the characteristic load deflection curve parameters (including yield load, peak load, ultimate load and corresponding drift, ductility and post peak strength degradation) are very much essential for efficient design of these structures. Hence, extensive research has been conducted to develop robust simulation models to predict the behavior of RC hollow bridge piers [2, 3]. The classic finiteelement models based on fiber cross section and nonlinear beam-column elements developed by researchers [4] are widely used because they are very effective in predicting the flexural behavior of RC members under seismic loading [5]. However, these elements are not very effective in predicting the shear behavior of RC members. Hence, members subjected to shear and torsional loadings cannot be analyzed directly using the nonlinear beam-column elements. Indirect methods are necessary to predict the effect of shear and torsional loadings. The effects of shear and torsional loads can be incorporated into the 1D nonlinear beam-column elements either through kinematic assumptions, i.e. by considering shear deformation or by using multi-axial material constitutive laws in the formulation of the 1D elements. The first fiber element formulation which accounted for shear deformations was developed by Guedes and Pinto [6], by using the strut and tie approach (truss analogy) for the analysis and uniaxial

*Corresponding author. Tel: +918843970977; E-mail address: vijaypolimeru@gmail.com

© 2022 The authors. Published by Alwaha Scientific Publishing Services, ASPS. This is an open access article under the CC BY license.

Published online: December 19, 2022
doi:10.38208/acp.v1.502

constitutive laws for material nonlinearity. However, the developed formulation was unable to capture the coupled shear flexure behavior, strength and stiffness degradation and the pinching effect.

Ranzo and Petrangeli [7] developed a nonlinear beam-column element in which the section forces were related to the sectional deformations to incorporate axial shear flexure interaction. The shear force and deformation at a section of the element were coupled with axial and flexural forces using the sectional damage criteria developed by Priestley et al[8]. Similar to the other truss analogy approaches, the shear strength of the element was estimated as an algebraic sum of strengths of different mechanisms, i.e. direct coupling was not modelled. Petrangeli[9] proposed another flexibility based nonlinear fiber beam-column element using microplane models [10] to determine the multiaxial response of RC members. Biaxial constitutive relationships were implemented in the model to predict the response of RC members subjected to cyclic and monotonic loadings [11]. However, the formulation involved several computational complexities, which are difficult to implement in structural analysis software.Most of the above-mentioned methods involve damage parameters, which are non-physical and also not specified in any damage assessment and design codes [12,13,14]. The merits and demerits of these various models for analyzing the hollow bridge piers clearly emphasizes the need for development of more robust and rational analytical models which can accurately predict the load deformation parameters and the failure modes of hollow RC rectangular bridge piers.

Various rational analytical 2D models have been developed by researchers, over a span of forty years, to study the complete nonlinear behavior of RC wall type structures. These models include Modified Compression Field Theory (MCFT) [15], Rotating Angle Softened Truss Model (RA-STM) [16], Fixed Angle Softened Truss Model (FA-STM) [17], Disturbed Stress Field Model (DSFM) [18], Softened Membrane Model (SMM) [19] and Cyclic Softened Membrane Model (CSMM) [20]. From the literature, it is understood that, CSMM model developed by [20] using the smeared (average) crack approach in continuum mechanics, can rationally predict the concrete contribution to shear, capable of modelling the Poisson effect, pinching effects and post peak strength degradations in RC wall type structures under reversed cyclic loading over the other models. More information on the above-mentioned models in terms of their relative advantages and disadvantages can be found in [21, 22]. Mo et al.[23] incorporated CSMM model in the OpenSEES nonlinear finite element (NLFE) framework.

On the other hand, there has been a significant amount of research reported in the development of analytical models for predicting the behavior of RC bridge piers [24]. Of these, the models based on fibersection analysis method are most commonly used [25].Primarily, this method involves two steps, first is evaluating the cross-sectional properties (such as neutral axis depth, moment and curvature (ϕ)) at a critical section and second, deriving load deflection curves from the derived cross-sectional properties. Jirawattanasomkul[24] and Mo [26] reported various approaches available in the literature to derive the load deflection relationships from cross sectional properties.

It has been understood from literature review, that there is a research gap pertaining to the relative efficiencies of these 1D, 2D and analytical models in predicting the response of hollow RC bridge piers under monotonic loadings. Hence, a comparative study has been performed to address the research gap. A nonlinear static pushover analysis of three hollow rectangular RC bridge piers (one flexure critical and two shear critical) has been performed under monotonic loading using four different analysis techniques. The first type of simulation model used in the present study (denoted as NLBC) is based on the commonly used fiber based nonlinear beam-column elements with simple uniaxial material constitutive relationships, which are very effective in predicting the flexural response of bridge piers. The second type of simulation model used in the present study (denoted as HS-NLBC) is also based on simple fiber based nonlinear beam-column elements. However, the constitutive relationships of steel in this model are modified to predict the post-peak strength degradation in shear critical bridge piers. The third type of simulation model is based on two dimensional (2D) CSMM based smeared RC plane stress elements. This model denoted as CSMM. The fourth type of simulation model is an analytical model based on the sectional analysis method. This model is denoted as Analytical. In this model, the load deflection relationships have been derived from moment curvature relationships using the methodology developed by Mo [26] (Wherein, the deflection has been evaluated using curvature diagrams and lateral load has been evaluated from the moment).The relative efficiencies of the finite element and analytical models have been evaluated by comparing the load deflection curve properties (including yield load, peak load, ultimate load and corresponding drift, ductility and post peak strength degradation) as predicted by the respective models with each other and also with the experimental data.

2. Methodology

2.1. Specimen Description

The three RC hollow rectangular bridge piers analyzed in the present study (namely, PI1, PI2, and PS1) were tested under combined axial and reversed cyclic loading conditions. In the present study, the backbone curves of the hysteretic loops have been used for validating the finite element and analytical models under monotonic loadings. The geometric and material properties of the three piers are shown in Table 1. The first character ‘P’ of the specimen names stands for Prototype. The second character ‘I’ or ‘S’ of the specimen names stands for insufficient or sufficient shear reinforcement respectively, with reference to the shear reinforcement requirement as per ACI code [27]. The third character ‘1’ or ‘2’ of the specimen’s names stands for smaller or greater spacing of lateral reinforcement respectively. All information on the experimental setup, loading protocols, design details and failure modes of the three specimens have been reported by [28].

Table 1 Geometric and Material Properties of Bridge Piers

Specimen No. (Aspect Ratio)		PI1 (3.75)	PI2 (2.91)	PS1 (5.41)
$f_c^{'}$(Mpa)		34	32	34
N (kN)		4000	3600	4000
L(mm)		4500	3500	6500
Longitudinal Reinforcement	η (mm)	22	22	22
	f_{yl}(Mpa)	460	418	460
	ρ_l (%)	1.60	1.60	1.60
	f_{sul} (Mpa)	647	627	647
Transverse Reinforcement	ϕ(mm)	10	10	13
	f_{yt}(Mpa)	510	420	343
	ρ_t (%)	0.40	0.20	1.10
	Spacing (mm)	120	200	80

2.2. Finite Element Modelling

In the present study, two 1D fiber based and one 2D CSMM based finite element models has been used to evaluate the performance of the hollow rectangular bridge under monotonic loads. The first type of 1D model used in the present study is based on simple fiber based nonlinear beam-column elements with simple uniaxial material constitutive relationships, which is very effective in predicting the flexural response of bridge piers. This type of model is denoted as NLBC based model. The second type of 1D model used in the present study is also based on simple fiber based nonlinear beam-column elements. However, the constitutive relationships of steel in this model are modified to predict the hysteretic characteristics of shear critical bridge piers such as pinching effect and post-peak strength degradation. This type of model is denoted as HS-NLBC type model. The CSMM based 2D finite element model is denoted as CSMM based model. Finite element models of the piers have been developed using OpenSEES software. Post processing of the analysis results have been performed using MATLAB software.Each bridge pier has been modelled as a cantilever using displacement based nonlinear beam column elements in the NLBC and HS-NLBC simulation models. The cross section of each element has been discretized into several concrete and steel fibers, with appropriate nonlinear material constitutive models assigned to each of the steel rebar fibers as well as the confined and unconfined concrete fibers. The discretization approach followed in the CSMM simulation model is slightly different from that of the NLBC and HS-NLBC models. The walls of the bridge piers parallel to the bending direction are more shear critical in nature compared to the walls perpendicular to the bending direction [28]. Hence the walls of the bridge piers parallel to the bending direction have been modelled using CSMM based four node smeared RC plane stress elements in the CSMM model.The accuracy of any finite element analysis results depends a lot on the mesh size, type of elements and the type of boundary conditions imposed. A critical convergence study has been performed to select the number of elements in both 1D and 2D models. The parameters considered for the convergence study are the hysteretic load displacement response and stresses and strains at the critical sections. After a detailed convergence study, 20 nonlinear beam-column elements have been used in the 1D models of the bridge piers. The cross section of each element is further divided into 10 confined, 10 unconfined concrete and 64 steel fibers. On the other hand, 2D analysis has been performed with 20 nonlinear beam-column elements in each of the two walls (aligned perpendicular to the bending direction) with 4 unconfined concrete, 10 confined concrete, 32 steel rebar fibers each. 40 CSMM based plane stress elements have been used for modelling the other two bridge piers walls (aligned parallel to the bending direction). More information on the finite element modelling of the bridge piers has been reported inPolimeru and Laskar[29]. The lateral loading histories under which the individual bridge piers we analysed are simple monotonic loadings with peak amplitudes of 196mm for PI1, 80mm for PI2 and 420mm for PS1.

2.3. Analytical Modelling

Fig. 1, presents the pseudocode of the methodology followed to evaluate moment (M) curvature (ϕ) and lateral load (P) deflection (Δ) curve of the hollow rectangular bride piers for one bending strain value ($\varepsilon_{bending}^{i}$). In the present study, the hollow section, has been idealized as an equivalent I section as shown in Fig. 2. This methodology, primarily involves to seven key functions. *PrepareFiberCrossSection*, this function discretizes the cross section into several concrete and steel layers (or fibers) as shown in Fig. 3. Assume initial value of normal bending strain $\varepsilon_{bending}^{i}$ in the extreme concrete fibre. Then, Calculate the total strain by adding the bending strain and axial strain due to applied axial loading (i.e. $\varepsilon_{total}^{i} = \varepsilon_{axial} + \varepsilon_{bending}^{i}$) and assume a trial neutral axis depth, then using *CalculateStrainsInAllFibers* function evaluate the strains in all steel and concrete fibers using linear distribution of strain over the cross-section and compatibility of strains in adjacent steel and concrete layers. Then, calculate stresses in all the steel and concrete fibres using corresponding constitutive relationships of steeland concrete using *CalculateStressesInAllFibers*function. In the presentstudy, the constitutive models of concrete formulated by Chang and Mander[30] and Steel formulated by Mansour [20] has been used. Then, using *CalculateForcesInAllFibers* function, the forces in each fiber has been evaluated by multiplying the fiber stress with the cross-sectional area of the fiber. Then the, net axial load will be evaluated and compares with the prescribed tolerance (tol) limit, if the net axial load is greater than the tolerance, then iteration will continue with a new neutral axial depth (NA_i). In the present study, a simple function *UpdateNADepth*, has been written based on Intermediate value theorem [31], has been developed in Matlab. If the net axial load is less than the tolerance, then the iteration will be aborted and the moment curvature and load deflection values will be evaluated using *evaluateMomentCurvture* and *evaluateLoadDeflection* functions.

Algorithm 1: Evaluation of Moment Capacity (M), Curvature (ϕ), Lateral Force (P) and Lateral deflection(Δ) of Bridge Piers

Input : L, H, l_f, H_f, l_w, H_w, ρ_l, Φ, f_{ck}, f_y, N, to, $\varepsilon^i_{bending}$
Output: NA, M, ϕ, P, Δ

```
C = 0
T = 0
NetAxialLoad = abs(C-T-N)
NA_i = n
PrepareFiberCrossSection()
while NetAxialLoad > tol do
    ε_fiber = calculateStrainsInAllFibers(NA_i)
    σ_fiber = calculateStressesInAllFibers(ε_fiber)
    [C, T] = calculateForcesInAllFibers(σ_fiber)
    NetAxialLoad = abs(C-T-N)
    NA_i = UpdateNADepth()
end
NA = NA_i
[M, φ] = evaluateMomentCurvature(NA)
[P, Δ] = evaluateLoadDeflection(NA, M, φ)
```

Fig. 1. Pseudocode Describing the Evaluation Procedure of Moment Capacity, Curvature, Lateral Force and Deflection of RC Hollow Rectangular Bridge Piers

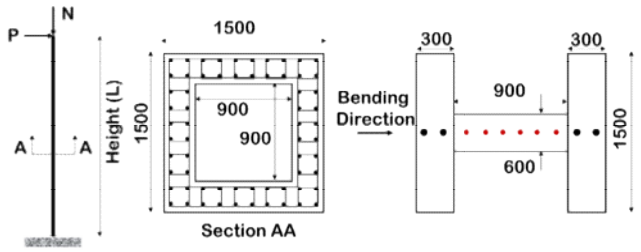

Fig. 2. Cross Section and Elevation of Bridge Piers

2.3.1. Evaluation of Moment Curvature

The calculation of moment capacity (M) and curvature (φ) of the section depends on the position of the neutral axis. When the neutral axis lies inside the section as shown in Fig. 3, $M-\varphi$are calculated using Eqns 1 and 3. When neutral axis lies outside the section as shown in Fig. 4, $M-\varphi$ are calculated using Eqns 2 and 3.

$$M = F_C * y_{comp} + F_t * y_{Tensile} \quad (1)$$

$$M = F_C * y_{\text{comp}} \quad (2)$$

$$\phi = \varepsilon_{bending}/NA \quad (3)$$

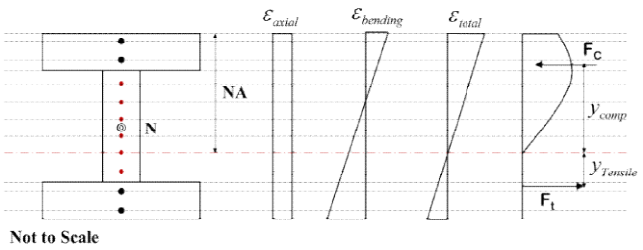

Fig. 3. Stress-Strain Distribution with Neutral Axis Inside Pier Section

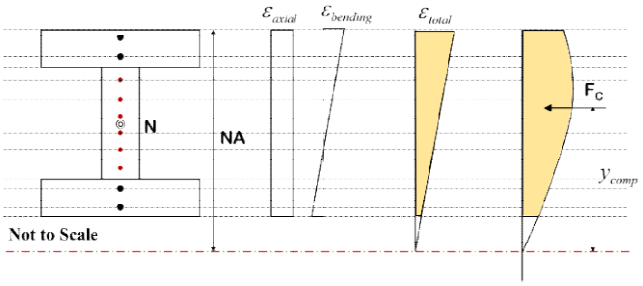

Fig. 4. Stress Strain Distribution with Neutral Axis Outside Pier Section

2.3.2. Evaluation of Load deflection curves

The load and corresponding deflection in the ascending branch of the load-deflection curves of the bridge piers have been calculated from the curvature diagrams corresponding to three stages of the piers, namely up to cracking, between cracking and yielding and between yielding and peak. The calculation procedures used in the individual stages of the piers are discussed below.

2.3.2.1. Ascending Branch

Upto Cracking - The curvature diagram of the pier at the initiation of cracking shown in Fig. 5, has been used to calculate the deflection of the pier at crack initiation. The load and deflection of the pier up to cracking have been calculated using Eqns4 and 5 respectively. Moment and curvature at the base of pier at crack initiation ($M_{cr}-\varphi_{cr}$) have been calculated corresponding to the cracking strain of concrete given in Eqn 6.

$$P = \frac{M}{L} \quad (4)$$

$$\Delta = A\left(\frac{2L}{3}\right) = \left(\frac{1}{2}\varphi L\right)\left(\frac{2L}{3}\right) \quad (5)$$

$$\varepsilon_t = \frac{f_t}{E_C} \quad (6)$$

where $f_t = 0.7\sqrt{f_c'}$ and $E_c = 5000\sqrt{f_c'}$

Between Cracking and Yielding - The curvature diagram of the pier at the initiation of yielding of the reinforcement, shown in Fig. 6, has been used to calculate the deflection of the pier at the yielding of the reinforcement. The deflection of the pier between crack initiation in concrete and yielding of reinforcement have been calculated using Eqn7. Moment and curvature at the base of pier at the initiation of the yielding of the reinforcement ($M_y-\varphi_y$) have been calculated at the yield strain of the reinforcement.

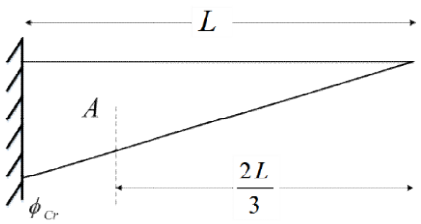

Fig. 5. Curvature Diagram of Bridge Pier Upto Cracking

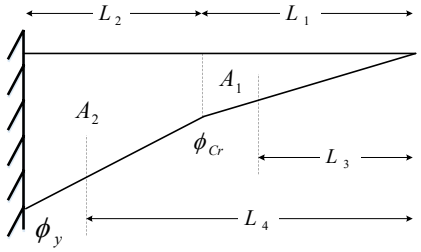

Fig. 6. Curvature Diagram of Bridge Pier Upto Yielding

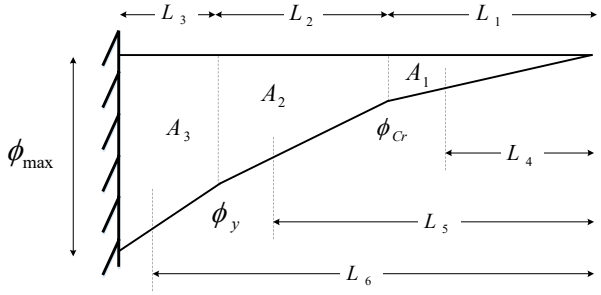

Fig. 7. Curvature Diagram of Bridge Pier Up To Peak

$$\Delta = A_1 L_3 + A_2 L_4$$
$$\Delta = \left(\frac{1}{2}\varphi_{cr} L_1\right) L_3 + \frac{L_2}{2}(\varphi_{cr} + \varphi) L_4 \qquad (7)$$

Between Yielding and Peak - The curvature diagram of the pier at the peak load, shown in Fig. 7, has been used to calculate the deflection of the pier at the peak load. The deflection of the pier between the yielding of reinforcement and the peak load has been calculated using Eqn8. Moment and curvature at the base of pier at the peak load ($M_{max} - \psi_{max}$) have been calculated at the ultimate strain of concrete.

Where , $L_1 = \frac{M_{cr}}{M_{max}} L$, $L_2 = \frac{M_y}{M_{max}} L$, $L_3 = L - L_1 - L_2$ and L_4, L_5, L_6 distances from the free end to the CGs of areas A_1, A_2 and A_3 respectively under the curvature diagram shown in Fig. B.7.

$$\Delta = A_1 L_4 + A_2 L_5 + A_3 L_6$$
$$\Delta = \left(\frac{1}{2}\phi_{cr} L_1\right) L_4 + \frac{L_2}{2}(\phi_{cr} + \phi_y) L_5 \qquad (8)$$
$$+ \frac{L_3}{2}(\phi_{cr} + \phi) L_6$$

2.3.2.2. Descending Branch

In the descending branch, the elastic restoration and reloading curvature diagrams of the pier, shown in Fig.s 8 and 9, have been used to calculate the deflection of the pier in the post-peak region of the load deflection curve. The flexural rigidity of the pier during elastic restoration and reloading has been obtained from the moment curvature diagram of the pier shown in Fig. 10. The deflections of the pier due to elastic restoration and reloading have been calculated using Eqns9 and 10 respectively. The reloading curvature diagram of the pier between the base and the yield initiation point has been represented by a third order curve as shown in Fig. 11 and expressed in Eqns11 through 14. The overall deflection of the pier in the post peak region has been calculated using Eqn15.

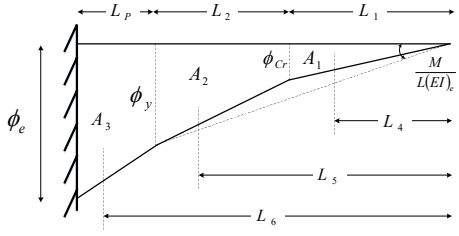

Fig. 8. Curvature Diagram of RC Hollow Bridge Pier Upto Elastic Restoration Curvature

Where, $\varphi_e = \left(\frac{M_{max}}{M_y}\right)\phi_y$, $L_1 = \frac{M_{cr}}{M_{max}} L$, $L_2 = \frac{M_y}{M_{max}} L$, $L_P = L - L_1 - L_2$ and L_4, L_5, L_6 are distances from free end to the CGs of areas A_1, A_2 and A_3 respectively under the curvature diagram shown in Fig. 8.

$$\Delta = A_1 L_4 + A_2 L_5 + A_3 L_6$$
$$\Delta = \left(\frac{1}{2}\phi_{cr} L_1\right) L_4 + \frac{L_2}{2}(\phi_{cr} + \phi_y) L_5 \qquad (9)$$
$$+ \frac{L_p}{2}(\phi_{cr} + \phi_e) L_6$$

Where, $\varphi_r = \varphi - \varphi_{max} + \phi_e$, $\varphi_{cr\_red} = \frac{M}{M_{max}}\phi_y$, $\varphi_{y\_red} = \frac{M}{M_{max}}\phi_y$, $L_1 = \frac{M_{cr}}{M_{max}} L$, $L_2 = \frac{M_y}{M_{max}} L$, $L_P = L - L_1 - L_2$ and L_4, L_5, L_6 are distances from free end to the CGs of areas A_1, A_2 and A_3 respectively under the curvature diagram shown in Fig. 10.

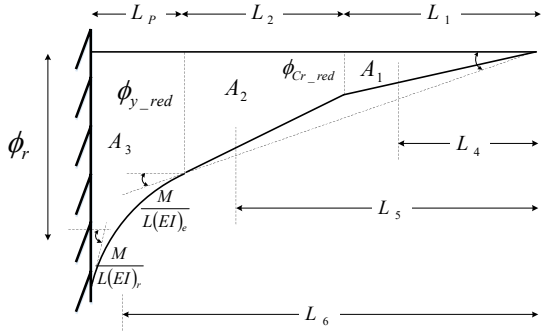

Fig. 9. Curvature Diagram of RC Hollow Bridge Pier Upto Reloading Curvature

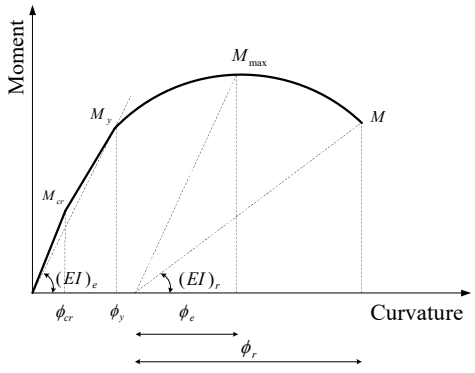

Fig. 10. Moment Curvature Diagram

$$\Delta = A_1L_4 + A_2L_5 + A_3L_6$$
$$\Delta = \left(\frac{1}{2}\phi_{cr}L_1\right)L_4 + \frac{L_2}{2}(\phi_{cr} + \phi_y)L_5 + A_3L_6 \quad (10)$$

A third order curve is fitted between φ_y and φ_r

$$\varphi = Ax^3 + Bx^2 + Cx + D \quad (11)$$

$$\theta = \frac{d\varphi}{dx} = 3Ax^2 + 2Bx + C \quad (12)$$

$$\text{At } x = 0,\ \varphi_{y\_red} = D \text{ and } \theta_{y\_red} = C \quad (13)$$

$$\text{At } x = L_P,\ \varphi_r = AL_P^3 + BL_P^2 + CL_P + D \text{ and } \theta_r = 3AL_P^2 + 2BL_P + C \quad (14)$$

Solving the above Eqns11 to 14 for coefficients A, B, C and D.

$$A = \frac{2\phi_{y\_red} - 2\phi_r + L_P\theta_r + L_P\theta_{y\_red}}{L_P^3}$$

$$B = \frac{-(3\phi_{y_{red}} - 3\phi_r + L_P\theta_r + 2L_P\theta_{y_{red}})}{L_P^2}$$

$$C = \theta_{y\_red} \text{ and } D = \phi_{y\_red}$$

Then the deflection can be calculated using Eqn15

$$\Delta_{Post-peak} = \Delta_{max} - \Delta_e + \Delta_r \quad (15)$$

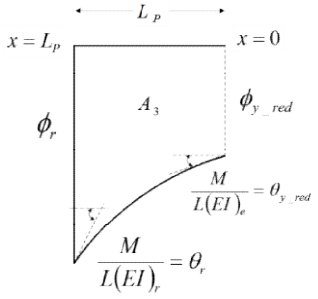

Fig. 11. Reloading Curvature

3. Results and Discussion

3.1. Load Displacement Curves

The backbone curves obtained from 1D, 2D and analytical models have been compared with the test results for all the three bridge piers PS1, PI1 and PI2 as shown in Fig.s 12 –14. Comparing the results obtained from 1D, 2D and analytical models developed in this study, it can be observed that,only CSMM and HS-NLBC models are able to simulate the descending branch of shear critical bridge piers PI1 (Fig. 12) as compared to the NLBC and analytical models. In the bridge pier, PI2, as shown in Fig. 13, the ascending and descending branches predicted by the 2D CSMM model are matching well with the experimental results compared to other 1D finite element and analytical models. The NLBC, CSMM and Analytical models are very effective in predicting the response of flexure critical bridge pier PS1 (Fig. 14).Since nonlinear beam-column elements with fibre section and analytical model are primarily effective in simulating the flexural behavior of the piers, these models are unable to accurately capture the post peak behavior in bridge piers PI1 and PI2. However, the 2D plane stress elements, based on the smeared crack approach, are capable of predicting both flexural and shear behavior. Though, HS-NLBC is capable of simulating the descending branch in all the three bridge piers, the efficiency of HS-NLBC simulation is highly dependent on the accurate calibration of calibrated pinching and damage properties. This calibration process is not a rational process, since it cannot be performed in the absence of test data.

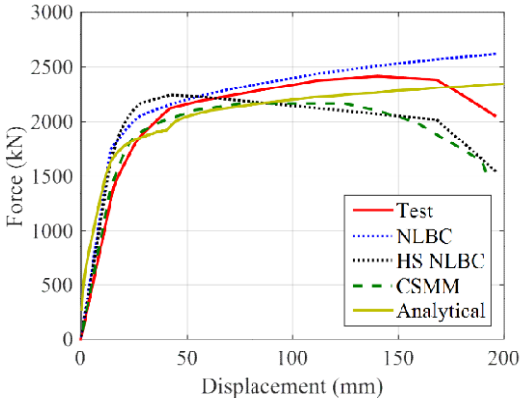

Fig. 12. Backbone Curves for Bridge Pier PI1

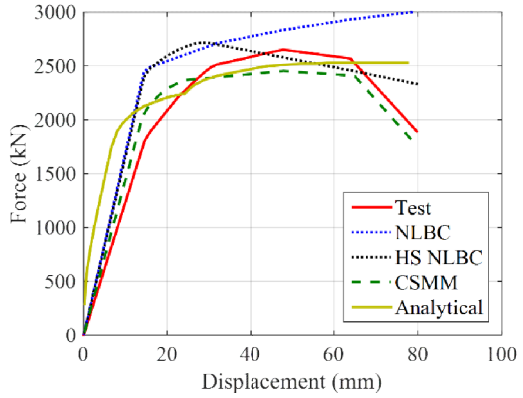

Fig. 13. Backbone Curves for Bridge Pier PI2

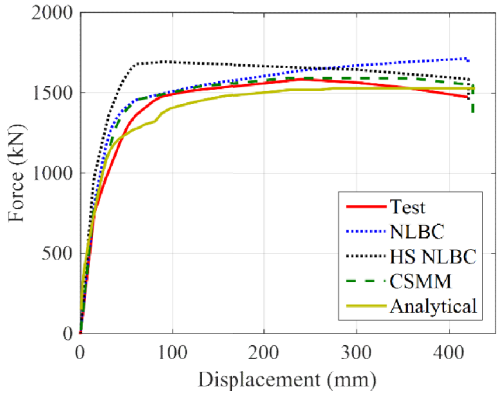

Fig. 14. Backbone Curves for Bridge Pier PS1

3.2. Backbone Curve Parameters

The primary backbone curve parameters obtained from experimental and simulation results are shown in Fig. 15, to 17. The yield displacement has been calculated as the displacement at the idealized strength of the piers [28] corresponding to an elastic stiffness equal to the mean secant stiffness at 75% of the idealized strength [32]. From the results, it can be observed that though the yield loads and yield drifts of the bridge piers PI1 and PS1 are well predicted by the 1D and 2D finite element models and the analytical model. However, the yield loads and yield drifts of the bridge pier PI2 are well predicted by the 1D and 2D finite element models compared to the analytical model. Peak loads, ultimate loads and corresponding drifts of all the three bridge piers are well captured by the 2D model compared to 1D and analytical models.

Also, in the 1D model and analytical models post peak strength degradation is not observed, i.e. no difference between the peak and ultimate loads is observed. The ductility results from 1D, 2D and analytical models are presented in Fig. 18, ductility values indicate nonlinear drift capabilities in pushing cycles. It can be observed from Fig. 18 that the ductility values predicted by the 2D model are closer to the experimental values of ductility in the shear critical bridge piers PI1 and PI2. The higher accuracy of the 2D model in predicting the yield loads, peak loads, ultimate

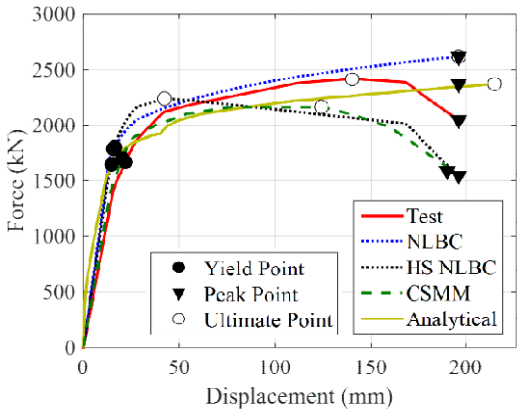

Fig. 15. Critical Loads for Bridge Pier PI1

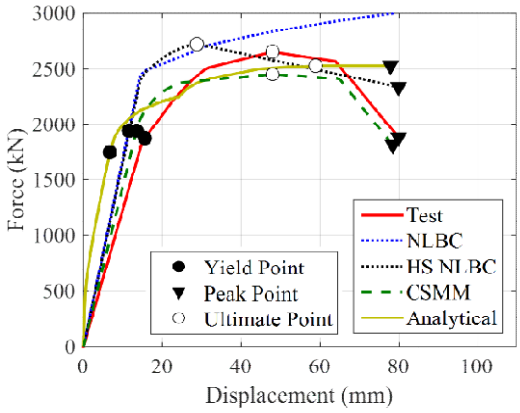

Fig. 16. Critical Loads for Bridge Pier PI2

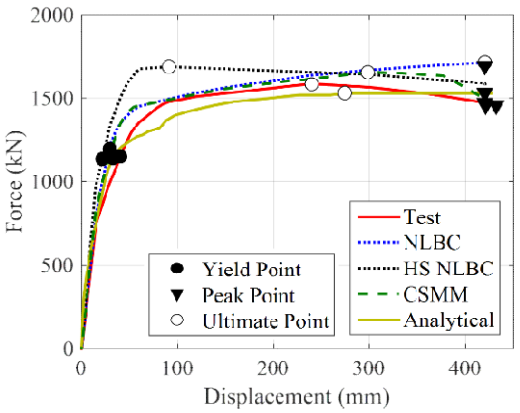

Fig. 17. Critical Loads for Bridge Pier PS1

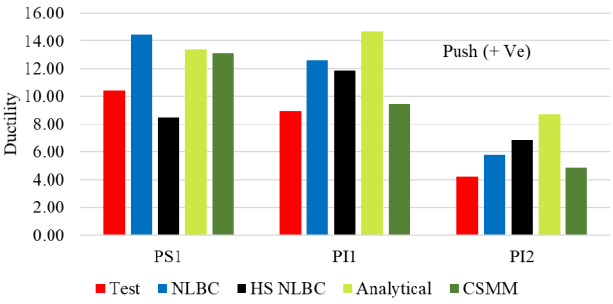

Fig. 18. Ductility of Bridge Piers

loads and corresponding drifts of the piers including post peak strength reduction is possible due to the use of 2D elements in modelling the shear critical walls of the bridge piers oriented along the loading direction

4. Conclusions

This paper evaluates the relative efficiencies of the finite element and analytical models by comparing the load deflection curve properties (including yield load, peak load, ultimate load and corresponding drift, ductility and post peak strength degradation) as predicted by the respective models under monotonic loading with each other and also with the experimental data. From the analysis results, it is observed that, the 2D CSMM model is able to accurately capture the response of ascending and descending branches in all the three bridge piers. Though the yield loads and corresponding drifts are well predicted by all the three finite element models of all the three bridge piers, the peak, ultimate loads and corresponding drifts are well predicted by the 2D CSMM model compared to 1D finite element and analytical models. Similarly, the ductility values predicted by the 2D CSMM model of shear critical bridge piers (PI1 and PI2) are corroborating well with the experimental data, compared to the 1D finite element and analytical models.It can thus be concluded that the 2D CSMM based finite element model is very robust and effective in predicting the load deformation characteristics of flexure as well as shear critical bridge piers with reasonable accuracy over 1D

(NLBC and HS-NLBC) and analytical models investigated in this study.

Acknowledgements

This research was funded by Grant No. 14IRTAPSG011 from Industrial Research and Consultancy Centre (IRCC) at Indian Institute of Technology Bombay. The support is gratefully acknowledged. The RC bridge pier specimens analyzed in this manuscript have been tested at the National Center for Research in Earthquake Engineering, Taiwan. The authors sincerely thank Dr. Y.L. Mo for providing the test results

Nomenclature

C and T	Total Compression and Tensile forces in all fibers
L and H	Height and width of the pier
L_f and H_f	Height and width of equivalent flanges of I section
N	Sustained Axial load
f_c'	Compressive strength of concrete
f_{yl} and f_{yt}	Yield strengths of longitudinal and transverse reinforcement bars
η and ϕ	Diameters of longitudinal and transverse reinforcement bars
ρ_l and ρ_t	Percentage of longitudinal and transverse reinforcement

Disclosures

Free Access to this article is sponsored by SARL ALPHA CRISTO INDUSTRIAL.

References

1. CasseseP, Ricci P, Verderame GM. Experimental study on the seismic performance of existing reinforced concrete bridge piers with hollow rectangular section, Engineering Structures, 2017, 144: 88-106.
2. Li Z, Chen Y, Shi Y, Numerical failure analysis of a continuous reinforced concrete bridge under strong earthquakes using multi-scale models. Earthquake Engineering and Engineering Vibration, 2017; 16(2): 397-413.
3. Liu KY, Witarto W, Chang KC. Composed analytical models for seismic assessment of reinforced concrete bridge columns, Earthquake Engineering & Structural Dynamics,2015; 44(2): 265-281.
4. Spacone E, Filippou FC, Taucer FF, Fibre beam-column model for nonlinear analysis of R/C frames: Part I. formulation. Earthquake Engineering and Structural Dynamics,1996; 25(7): 711–725.
5. Ceresa P, Petrini L, Pinho R. Flexure-shear fibre beam-column elements for modeling frame structures under seismic loading—state of the art. Journal of Earthquake Engineering, 2007; 11(S1): 46-88.
6. GuedesJ, Pinto AV. A numerical model for shear dominated bridge piers. Proceedings of the Second Italy-Japan Workshop on Seismic Design and Retrofit of Bridges, Rome, Italy, 1997.
7. Ranzo G, Petrangeli M. A fibre finite beam element with section shear modelling for seismic analysis of RC structures. Journal of Earthquake Engineering,1998; 2(3): 443–473.
8. Priestley MJN, Verma R, Xiao Y, Seismic shear strength of reinforced concrete columns. Journal of Structural Engineering, ASCE, 1994; 120(8): 2310–2329.
9. Petrangeli M, Modellinumerici per strutturemonodimensionali in cementoarmato, Ph.D. thesis, Università di Roma La Sapienza, Roma, Italy, 1996.
10. Bazant ZP, Oh BH. Microplane model for progressive fracture of concrete and rock. Journal of Engineering Mechanics, 1985,ASCE, 111(4): 559–582.
11. Petrangeli M, Pinto PE, Ciampi V, Fibre element for cyclic bending and shear of RC structures. I: theory. Journal of Engineering Mechanics, ASCE, 1999; 125(9): 994-1001.
12. Ko YF, Phung C, Nonlinear static cyclic pushover analysis for flexural failure of reinforced concrete bridge columns with combined damage mechanisms, Acta Mechanica, 2014; 225(2): 477-492.
13. Kashani MM, Lowes LN, Crewe AJ, Alexander NA. Nonlinear fibre element modelling of RC bridge piers considering inelastic buckling of reinforcement, Engineering Structures, 2016a; 116:163-177.
14. Kashani MM, Lowes LN, Crewe AJ, and Alexander NA. Computational modelling strategies for nonlinear response prediction of corroded circular RC bridge piers", Advances in Materials Science and Engineering, 2016; 1:1-15.
15. Vecchio FJ, and Collins MP. The modified compression-field theory for reinforced concrete elements subjected to shear. Journal Proceedings of the American Concrete Institute, 1986; 83(2): 219-231
16. Hsu TTC, Softened truss model theory for shear and torsion. Structural Journal of the American Concrete Institute, 1988; 85(6):624-635.
17. Pang XBD, Hsu TTC.Behavior of reinforced concrete membrane elements in shear. Structural Journal of the American Concrete Institute, 1995; 92(6):665-679.
18. Vecchio FJ. Disturbed stress field model for reinforced concrete: formulation, Journal of Structural Engineering, ASCE, 2000; 126(9): 1070-1077
19. Hsu TTC, Zhu RRH. Softened membrane model for reinforced concrete elements in shear. Structural Journal of the American Concrete Institute, 2002; 99(4): 460-469.
20. Mansour M., Behavior of reinforced concrete membrane elements under cyclic shear: experiments to theory. Ph. D. Dissertation, Department of Civil and Environmental Engineering, University of Houston, Houston, TX, 2001.
21. Hsu TTC. Discussion of Disturbed Stress Field Model for Reinforced Concrete: Formulation by FJ Vecchio. Journal of Structural Engineering, 2002; 128(11): 1487-1488.
22. Vecchio FJ. Closure: Disturbed stress field model for reinforced concrete: formulation, Journal of Structural Engineering, 2002; 128(11): 1488-1489
23. Mo YL, ZhongJ, Hsu TTC. Seismic simulation of RC wall-type structures, Engineering structures, 2008; 30(11): 3167-3175.
24. Jirawattanasomkul T, Dawei Z, Ueda T. Prediction of the post-peak behavior of reinforced concrete columns with and without FRP-jacketing. Engineering structures, 2013; 56: 1511-1526.
25. Pešić N, Pilakoutas K. Flexural analysis and design of reinforced concrete beams with externally bonded FRP reinforcement. Materials and structures, 2005; 38(2): 183-192.
26. Mo YL, Dynamic behavior of concrete structures, 2013, 44. Elsevier.
27. ACI Committee 318., Building code requirements for reinforced concrete (ACI 318-95) and commentary, American Concrete Institute, International Organization for Standardization, 1995.
28. Yeh YK, Mo YL, Yang CY. Full-scale tests on rectangular hollow bridge piers. Materials and Structures, 2002; 35(2): 117-125.
29. Polimeru VK, Laskar A. Robustness evaluation of CSMM based finite element for simulation of shear critical hollow RC bridge piers. Engineering Computations, 2019;37(1): 313-344

30. Chang GA, Mander JB. Seismic energy-based fatigue damage analysis of bridge columns: Part I-Evaluation of seismic capacity, 1994, Buffalo, NY: National Center for Earthquake Engineering Research.

31. Walk SM. The Intermediate Value Theorem Is NOT Obvious—and I Am Going to Prove It to You. The College Mathematics Journal, 2011; 42(4): 254-259.

32. Zahn FA, Park R, Priestley MJN. Flexural strength and ductility of circular hollow reinforced concrete columns without confinement on inside face, Structural Journal of American Concrete Institute, 1990; 87(2): 156-166.